



Effect of contact geometry, loading, material properties and relative slip on the fretting fatigue behaviour of metallic components

Andrea Zanichelli, Andrea Carpinteri, Camilla Ronchei, Daniela Scorza

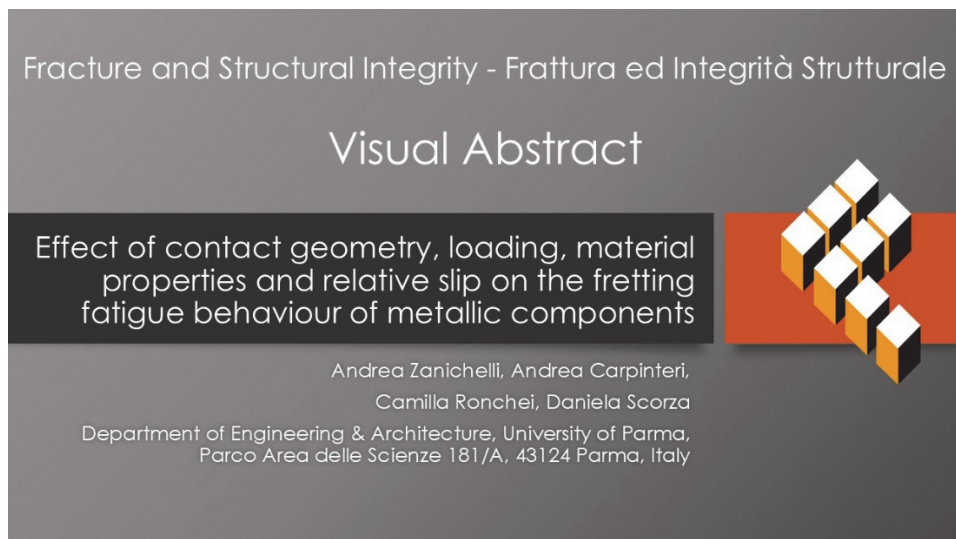
Department of Engineering & Architecture, University of Parma, Parco Area delle Scienze 181/A, 43124 Parma, Italy

andrea.zanichelli@unipr.it, <http://orcid.org/0000-0003-4152-8998>

andrea.carpinteri@unipr.it, <http://orcid.org/0000-0002-8489-6005>

camilla.ronchei@unipr.it, <http://orcid.org/0000-0001-5450-4448>

daniela.scorza@unipr.it, <http://orcid.org/0000-0001-2345-6789>



Citation: Zanichelli, A., Carpinteri, A., Ronchei, C., Scorza, D., Effect of contact geometry, loading, material properties and relative slip on the fretting fatigue behaviour of metallic components, *Fracture and Structural Integrity*, 72 (2025) 225-235.

Received: 24.02.2025

Accepted: 20.03.2025

Published: 23.03.2025

Issue: 04.2025

Copyright: © 2025 This is an open access article under the terms of the CC-BY 4.0, which permits unrestricted use, distribution, and reproduction in any medium, provided the original author and source are credited.

KEYWORDS. Al-4Cu alloy, Analytical methodology, Critical direction method, Critical plane-based criterion, Fretting fatigue.

INTRODUCTION

Fretting fatigue is a critical phenomenon that occurs in metallic components subjected to cyclic loading and small amplitude oscillatory motion at the contact interface. This phenomenon has garnered significant attention from researchers and engineers due to its detrimental impact on the structural integrity of various mechanical systems, including aircraft, turbines, and biomedical implants. In fact, numerous catastrophic failures have been attributed to fretting fatigue, such as the failure of dovetail joints in jet engine blades, leading to engine shutdowns, or the unexpected cracking of biomedical implants, which can compromise patient safety. Additionally, fretting fatigue was implicated in the collapse of critical bridge structures. Accordingly, understanding the mechanisms of fretting fatigue is essential for designing durable components and developing effective mitigation strategies.



The foundational understanding of the fretting phenomenon is due to the notable works by Tomlinson [1] and Waterhouse and Lindley [2]. In particular, the damage induced by fretting manifests itself as surface wear, cracks, and debris formation, which can act as stress concentrators, significantly reducing the fatigue life of the material. Since these early discoveries, numerous studies have been conducted to elucidate the complex interplay of mechanical, material, and environmental factors that govern the fretting fatigue behaviour.

One of the pioneering studies in fretting fatigue was conducted by Mindlin [3], who developed a theoretical framework to describe the stick-slip behaviour at contact interfaces. This work laid the groundwork for subsequent investigations into the stress distributions and crack nucleation mechanisms associated with fretting. In the following decades, researchers such as Hills and Nowell [4] advanced the understanding of fretting fatigue by employing finite element models to simulate contact mechanics and predict crack propagation pathways.

Based on the numerous studies carried out in this field, it is possible to state that fretting fatigue is influenced by a myriad of factors [5-7], which can be broadly categorized into: (i) the type of the contact and the fretting loading, (ii) the material properties, and (iii) the environmental parameters.

Relatively to the former group of influencing factors, the work of Majzoobi and Abbasi [8] provided a comprehensive analysis of the effects of contact geometry and load distribution, emphasizing how stress singularities at the edges influence crack nucleation. Further, particular attention has been paid to the effects of the contact pressure and the amplitude of relative motion: high contact pressure and small oscillatory displacements exacerbate the stress concentrations at the interface, promoting crack initiation [9]. For instance, Duquette [10] demonstrated the critical role of contact pressure in the nucleation of fretting cracks, emphasizing the importance of surface conditions. Moreover, the study by Hills [11] explored the influence of tangential forces on fretting crack propagation, showing a direct correlation between slip amplitude and crack growth rate. More recently, Su et al. [12] developed an estimation method for relative slip in fretting fatigue contact using digital image correlation, providing a novel approach to quantify slip and its effects on crack initiation.

Relatively to the material properties, harder materials are generally more resistant to wear but may exhibit higher susceptibility to crack initiation due to reduced plastic deformation capacity. Moreover, the work of Chen et al. [13] provided insights into the influence of microstructural variations on crack propagation paths in fretting fatigue scenarios. Further, the role of grain size in determining the fatigue life of materials has been highlighted [7], showing that finer grains improve crack resistance by enhancing plasticity. In another study, Santos et al. [14] examined the effects of heat treatment on alloy performance, finding that optimized heat treatment can significantly enhance hardness and reduce crack growth rates. Surface roughness also influences the distribution of contact stresses, with rougher surfaces being more prone to localized stress concentrations. In this regard, the development of surface treatments and coatings have demonstrated promising results in mitigating fretting-induced damage. For instance, surface treatments such as shot peening, laser shock peening and laser cladding can enhance fatigue resistance by inducing compressive residual stresses and improving surface hardness [15].

Environmental factors, such as temperature, humidity, and the presence of corrosive agents, further complicate the fatigue process [16]. Elevated temperatures can accelerate material degradation and alter the contact mechanics, while corrosive environments exacerbate crack propagation through stress-corrosion mechanisms. Recent studies have delved deeper into the impact of environmental parameters on fretting fatigue. Rustamov et al. [17] explored the synergistic effects of temperature and humidity on fretting fatigue behaviour, highlighting complex environmental interactions. Song et al. [18] investigated the fretting wear behaviour of electrical contacts under vacuum and atmospheric conditions, revealing that atmospheric exposure leads to severe surface oxidation and increased wear due to the formation and subsequent damage of oxide layers. Similarly, a comprehensive review by Li et al. [19] discussed the influence of temperature and humidity on fretting fatigue, underscoring the necessity for tailored protective measures in different service environments.

Despite the advancements gained in the last decades in the understanding of fretting fatigue, challenges still remain in developing universally applicable models for fretting fatigue due to the complex and multiscale nature of the phenomenon. In particular, the analytical and numerical approaches nowadays available need to be applied to several fretting configurations characterised by different contact types, fretting loading, material properties, and environmental conditions, in order to demonstrate to be suitable for a wide range of fretting fatigue problems.

In such a context, an analytical methodology, recently proposed by the present authors [20] to estimate both crack orientation and fatigue life of metallic structural components under constant amplitude fretting fatigue loading, is applied in the present paper. Firstly, a comprehensive experimental campaign available in the literature [21] is examined. These experimental tests, carried out on an aluminium alloy in partial slip regime by using two cylindrical fretting pads pushed against a dog bone specimen, are simulated by means of the above analytical methodology. Subsequently, a parametric analysis is carried out to assess the role of different influencing factors in affecting the fretting fatigue behaviour when such



a methodology is employed. In particular, valuable insights into the effects of such factors on both crack orientation and fatigue life are obtained.

ANALYTICAL METHODOLOGY FOR FATIGUE ASSESSMENT OF FRETTING-AFFECTED COMPONENTS

An analytical methodology, recently proposed for estimating both the crack nucleation orientation and the fatigue life of fretting-affected metallic structural components [20], is here employed to perform the fatigue assessment of such components. The key phases of the present analytical methodology are outlined below.

Firstly, the parameters used as input data for the methodology need to be set. In particular, this involves defining: (a) the type of contact, the radius of the pads, and the thickness and width of the specimen; (b) the mechanical and fatigue properties of the material, the friction coefficient, and the average grain size; and (c) the loading conditions (i.e. the normal load, the amplitude of the cyclic tangential load, and both amplitude and mean value of the bulk load).

Next, the stress distribution near the contact area is computed within the specimen, through either numerical simulations or analytical solutions for specific configurations, such as cylindrical or spherical contact pads. It is important to note that, in this study, the analytical solution related to cylindrical contact conditions [22] is implemented in the adopted methodology, in accordance with the configuration of the experimental fretting setup examined. This implies that the width of the contact area is determined by means of the Hertzian theory [22], as well as the contact pressure distribution between the specimen and the pads. Moreover, the solution proposed by Mindlin [3], modified in the way suggested by Hills and Nowell [4] in order to take into account the effect of the bulk stress, is employed to evaluate the width of the inner stick zone and the contact shear distribution. Then, the stress tensor in the vicinity of the contact zone can be computed by superimposing the stress contributions due to the constant normal load and the cyclic tangential load, with the bulk stress.

Once the stress field has been determined, the location of the hot-spot, H , on the contact surface is identified. More specifically, H is defined as the point where the highest value of the average maximum principal stress occurs. In the case of Hertzian contacts, either cylindrical or spherical, this point is found at the trailing edge of the contact area.

Subsequently, a procedure based on the Critical Direction Method [23] in combination with the Carpinteri et al. criterion [24] is exploited to determine the orientation of the critical plane. Such a procedure consists in taking into account a pencil of material planes passing through the hot-spot, each of them characterised by an orientation θ . Note that this system is characterized by a plane strain condition and may be consequently considered as a bi-dimensional problem. Accordingly, by taking in mind a bi-dimensional representation, each of the abovementioned material planes coincides with a segment, starting from H and having length equal to $2d$, being d the average material grain size. In such a way, the material microstructure is taken into account in the fretting fatigue assessment. Then, the value of a suitable fatigue parameter, defined according to the Carpinteri et al. criterion, is computed for each orientation considered. Such a fatigue parameter is the equivalent stress amplitude, $N_{eq,a}$, defined as follows:

$$N_{eq,a} = \bar{N}_a(\theta) + \sigma_{af,-1} \left(\frac{\bar{N}_m(\theta)}{\sigma_u} \right) \tag{1}$$

where $\bar{N}_a(\theta)$ and $\bar{N}_m(\theta)$ are the amplitude and the mean value, respectively, of the stress component normal to the critical plane averaged along the segment with orientation θ , whereas $\sigma_{af,-1}$ is the fatigue strength under fully reversed normal loading, and σ_u is the ultimate tensile strength.

The specific orientation, θ_{crit} , that maximizes the chosen fatigue parameter is selected as the critical plane and represents the predicted crack nucleation orientation.

Finally, the analytical fatigue life, $N_{f,cal}$, is computed according to the Carpinteri et al. criterion [24] through the following equation:

$$\sigma_{eq,a} = \sqrt{\left(N_{eq,a}\right)^2 + \left(\frac{\sigma_{af,-1}}{\tau_{af,-1}}\right)^2 \left(\frac{N_{f,cal}}{N_0}\right)^{2m} \left(\frac{N_0}{N_{f,cal}}\right)^{2m^*}} C_a^2 = \sigma_{af,-1} \left(\frac{N_{f,cal}}{N_0}\right)^m \tag{2}$$



where $\tau_{af,-1}$ is the fatigue strength under fully reversed shear loading, N_0 is the reference number of loading cycles for the definition of the fatigue strengths, m and m^* are the slopes of the S-N curves under fully reversed normal and shear stress, respectively, and C_a is the amplitude of the shear stress component lying on the critical plane.

It is worth noting that the fretting fatigue assessment is performed at the so-called critical point, P_{crit} , located at the endpoint of the segment with length of $2d$, oriented at an angle θ_{crit} with respect to the material surface. This segment originates from the hot-spot, which is identified as the crack nucleation site. Moreover, the stress components used in Eqn. (2) are based on the assumption that the critical plane orientation remains constant and equal to θ_{crit} .

EXPERIMENTAL CAMPAIGN ANALYSED

An experimental campaign reported in the literature [21], involving Al-4Cu specimens subjected to cylindrical fretting contact, is examined in the present research work by means of the analytical methodology described in the previous Section. The main features of such an experimental campaign are hereafter summarised.

The experimental program involved fretting fatigue tests carried out in partial slip regime on flat dog-bone specimens. Both mechanical and fatigue properties of the aluminium alloy constituting the specimens are listed in Tab. 1. It is worth noting that the friction coefficient, μ , related to the slip zone has been estimated (see Tab. 1), through an expression derived by Hills and Nowell [4], starting from the measured mean value, $\mu_m=0.5$. Such a value was determined after the first thousand of cycles by sliding the pads for a certain small distance and recording the corresponding tangential force, and it is referred to the whole contact surface. Therefore, a correction is needed to distinguish the value within the slip zone (which is expected to increase, as a surface modification takes place in such a zone) from the local value of the friction coefficient within the central stick zone (which remains constant due to the absence of relative motion between the contact surfaces).

Material property	
Elastic modulus, E	74 GPa
Poisson's coefficient, ν	0.33
Ultimate tensile strength, σ_u	465 MPa
Friction coefficient, μ	0.75
Fully reversed normal stress fatigue limit (at $2 \cdot 10^6$ cycles), $\sigma_{af,-1}$	191 MPa
Fully reversed shear stress fatigue limit (at $2 \cdot 10^6$ cycles), $\tau_{af,-1}$	110 MPa
S-N curve slope under fully reversed normal stress, m	-0.11
S-N curve slope under fully reversed shear stress, m^*	-0.11

Table 1: Mechanical and fatigue properties of the Al-4Cu alloy.

Moreover, a microstructural analysis highlighted the presence of grains elongated along the longitudinal direction of the specimen, with an average material grain size, d , equal to $50 \mu\text{m}$ in the direction perpendicular to the specimen surface.

The fretting loading conditions were those typical of classical fretting fatigue testing (i.e. a constant normal load, and a cyclic tangential load in phase with a cyclic axial load, characterised by a null mean value), and are summarised in Tab. 2. Different combinations of the fretting loads were used to perform the tests. Accordingly, the specimens were divided into four groups, as highlighted in Tab. 2. For each specimen group, the radius of the cylindrical pads, R , was made to vary to investigate the influence of such a geometric parameter on the fatigue life, whereas the fretting loads were chosen in order to keep constant the maximum value of the normal pressure, p_0 , the ratio Q_a/P (being Q_a the amplitude of the alternating cyclic tangential load, and P the constant normal load) and the cyclic stress amplitude, $\sigma_{B,a}$.

The experimental number of loading cycles, at which each tested specimen broke, is listed in Tab. 2. Moreover, after the specimen failure, experimental cracks were observed. They were found to nucleate in the vicinity of the contact edge, characterised by a direction towards the centre of the contact. In particular, the orientation of the experimental cracks



(defined with respect to the perpendicular to the contact surface) was found to range between 18° and 32°, for the first few hundred microns. Then, the main crack further propagated almost perpendicular to the surface.

Group No.	Test No.	R [mm]	P [N/mm]	Q _a [N/mm]	σ _{B,a} [MPa]	N _{f,exp} [cycles]	N _{f,cal} [cycles]
1	T1	50	93	42	92.7	1.29E+06	2.37E+06
	T2	75	140	63		6.70E+05	1.23E+06
	T3	100	186	84		8.50E+05	8.05E+05
	T4	125	233	105		7.30E+05	6.00E+05
	T5	150	280	126		6.70E+05	4.80E+05
2	T6	37.5	58	26	92.7	4.04E+06	5.56E+06
	T7	50	77	35		1.50E+06	3.47E+06
	T8	75	116	52		8.00E+05	1.79E+06
	T9	100	155	70		6.10E+05	1.18E+06
	T10	125	193	87		1.24E+06	8.84E+05
	T11	150	232	104		6.90E+05	7.05E+05
3	T12	75	116	52	77.2	1.42E+06	1.25E+06
	T13	100	155	70		6.10E+05	8.83E+05
	T14	125	193	87		1.24E+06	7.05E+05
4	T15	125	136	61	61.8	1.57E+06	2.79E+06
	T16	150	163	74		1.23E+06	2.30E+06

Table 2: Radius of the pads, R; constant normal load, P; amplitude of the alternating cyclic tangential load, Q_a; amplitude of the alternating cyclic axial stress, σ_{B,a}; and experimental fatigue life, N_{f,exp}, of each test analysed [21]. The analytically calculated fatigue life, N_{f,cal}, is also reported.

EXPERIMENTAL VALIDATION OF THE ANALYTICAL METHODOLOGY

The analytical methodology for fretting fatigue described above is employed to simulate the experimental tests [21] related to Al-4Cu specimens, and the results obtained in terms of fatigue life and crack nucleation orientation are reported and discussed in the present Section.

Relatively to the fatigue life, the values calculated through the methodology, N_{f,cal}, are listed in Tab. 2 for each tested specimen. Moreover, such results are compared to the corresponding experimental findings in Fig. 1 (scatter band 2 is indicated with dashed lines), for each specimen group separately. Satisfactory estimations are obtained, as confirmed by the fact that 14 cases (over 16) fall within the scatter band 2.

In addition, the accuracy of the present methodology is quantified by computing the value of the root mean square error, T_{RMS} (please refer to Ref. [25] for the T_{RMS} computation), which is equal to 1.66.

Relatively to the crack nucleation orientation, the values computed by means of the present methodology for each test considered are listed in Tab. 3. Note that such values are obtained by assuming the hot-spot, H, located where the highest value of the average maximum principal stress occurs on the contact surface, that is, at contact edge.

Further, it is important to stress that these values (ranging from 6° to 11°) are related to a length of 100 μm, that is, 2d. Accordingly, they should be compared to the first part of the experimental crack paths, where the orientation ranges from 18° to 32°. Therefore, it can be stated that, although the orientation of the crack is predicted towards the centre of the contact zone in agreement with the experimental observations, the present methodology underestimates the real value of the crack nucleation orientation.

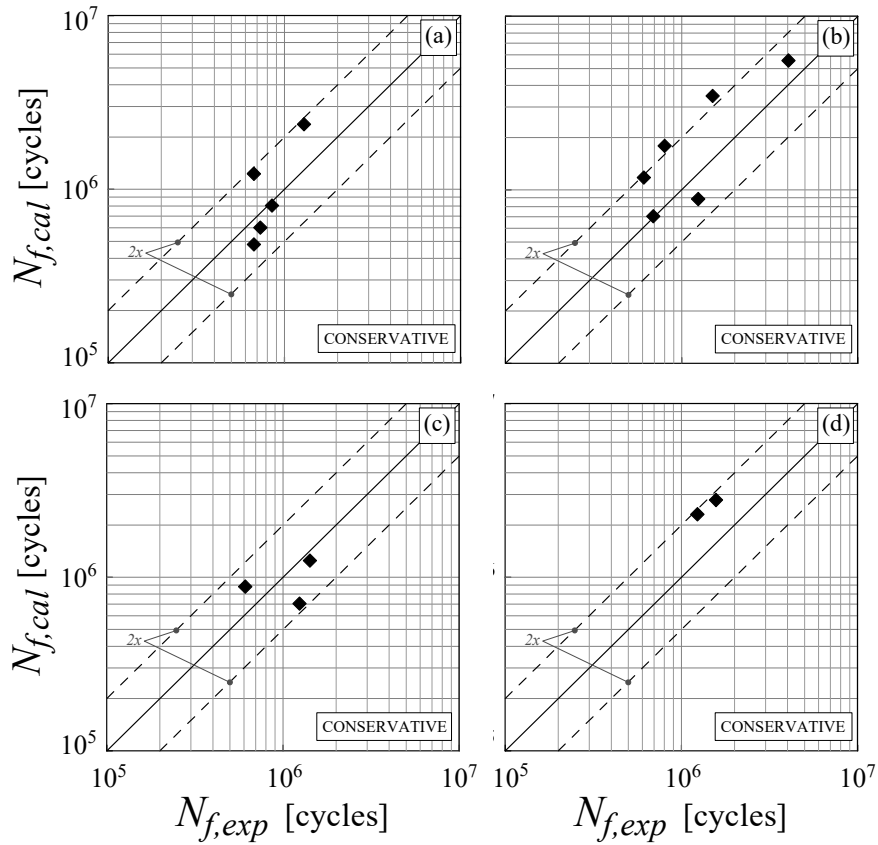


Figure 1: Comparison between analytical, $N_{f,cal}$, and experimental, $N_{f,exp}$, fatigue lives for specimen group: (a) No. 1, (b) No. 2, (c) No. 3, and (d) No. 4.

Group No.	Test No.	θ [°]	
		(H at contact edge)	(H at max Ruiz parameter)
1	T1	11	17
	T2	9	16
	T3	8	15
	T4	7	14
	T5	7	14
2	T6	11	17
	T7	10	16
	T8	9	15
	T9	8	14
	T10	7	14
	T11	7	14
3	T12	7	15
	T13	6	14
	T14	6	14
4	T15	6	15
	T16	6	15

Table 3: Crack nucleation orientation, θ , computed through the present methodology for each test considered, when the hot-spot, H , is assumed either at the contact edge or where the maximum value of the Ruiz parameter is attained.



INFLUENCE OF THE FRETTING PARAMETERS ON FATIGUE LIFE AND CRACK ORIENTATION

This Section is devoted to assess the role of different influencing factors in affecting the fretting fatigue behaviour when the present analytical methodology is employed. In particular, both fatigue life and crack nucleation orientation are computed for several fretting fatigue configurations, which are characterised by different parameters related to the contact geometry, the fretting loading, and the material properties.

Relatively to the contact geometry, it is well-known that the type of the contact influences the fretting fatigue behaviour. As a matter of fact, different solutions should be employed to analyse different contact types (one may think, for example, of the analytical solutions proposed by Hertz for the cases of cylindrical and spherical contact [22]). If the field of interest is narrowed to a specific case (that is, the cylinder-to-flat contact analysed in the present research work), the radius of the pad primarily affects the results significantly.

By considering a single specimen group analysed in the present work (that is to say, several tests characterised by different pad radii and the same values of maximum normal pressure, p_0 , ratio Q_a/P , and cyclic stress amplitude, $\sigma_{B,a}$), it is possible to observe that both the fatigue life (see Tab. 2 and Fig. 1) and the crack nucleation orientation (see Tab. 3) computed by the present methodology decrease as the pad radius increases. Note that this trend is also confirmed experimentally in terms of fatigue life (see Tab. 2), whereas no data are available in the original research work relatively to the relationship between the radius of the pad and the experimental crack nucleation orientation.

Now, in order to delve deeper into the effect on the fretting fatigue behaviour of different influencing factors, a reference condition is here defined and it will be hereafter considered. Such a condition corresponds to one of the experimental tests simulated in the previous Section, that is, the test No. T10. More precisely, it is characterised by: a radius of the pad of 125 mm; a constant normal load, a ratio between the cyclic tangential load amplitude and the normal load, and a cyclic axial stress amplitude equal to 193 N/mm, 0.45, and 92.7 MPa, respectively; a friction coefficient of 0.75; and an average material grain size equal to 50 μm .

As far as the fretting loads are concerned, different values and ratios obviously affect the stress state and, accordingly, the fatigue life. In such a context, the influence of the constant normal load, P (by changing the maximum value of the normal pressure, p_0), the amplitude of the cyclic tangential load, Q_a (by changing the ratio Q_a/P), and the amplitude of the cyclic axial stress, $\sigma_{B,a}$, on the fatigue life is investigated. In particular, one parametric analysis is performed for each of the three loading influencing factors and, more precisely:

- a parametric analysis is performed by varying P between 50 and 350 N/mm, whereas the values of Q_a/P and $\sigma_{B,a}$ are those of the reference condition;
- a parametric analysis is performed by varying Q_a/P between 0.1 and 0.7, whereas the values of P and $\sigma_{B,a}$ are those of the reference condition;
- a parametric analysis is performed by varying $\sigma_{B,a}$ between 20 and 140 MPa, whereas the values of P and Q_a/P are those of the reference condition.

The parameters related to the contact geometry and the material properties are those of the reference condition for each parametric analysis. The results of such analyses are shown in Figs. 2 (a), (b) and (c), respectively. It can be noted that the number of loading cycles to failure, $N_{f,calc}$, significantly decreases as the fretting loads increase. This trend is particularly pronounced when $\sigma_{B,a}$ is made to vary, highlighting that the amplitude of the cyclic axial stress is the most influencing parameter.

Moreover, the above decreasing trend seems to be also confirmed experimentally. As a matter of fact, by comparing the tests Nos T10 (corresponding to the reference condition) and T4 (characterised by the same fretting parameters of the reference condition, except for the constant normal load which is 21% higher than the reference one), it can be observed that the fatigue life of the latter is lower than that of the former (see Tab. 2). Moreover, by comparing the tests Nos T10 (corresponding to the reference condition) and T14 (characterised by the same fretting parameters of the reference condition, except for the amplitude of the cyclic axial stress which is 17% lower than the reference one), it can be observed that the fatigue life of the latter is higher than that of the former (see Tab. 2). The experimental fatigue life of tests Nos T10 and T4 are plotted in Fig. 2 (a), as well as that of tests Nos T10 and T14 in Fig. 2 (c).

Based on the above parametric analyses, no significant effect of the fretting loads on the crack nucleation orientation, θ , is found, with the exception of the case of $\sigma_{B,a}$. As a matter of fact, the orientation of the crack nucleation is estimated: equal to 5° independently of the value of P ; equal to 6° for Q_a/P up to 0.3, and 5° for bigger values. Moreover, as shown in Fig. 3, when $\sigma_{B,a}$ is made to vary between 0.0 and 157.5 MPa (this latter value identifying the limit for the partial slip condition), θ decreases, changing from 9° to 4° , respectively.

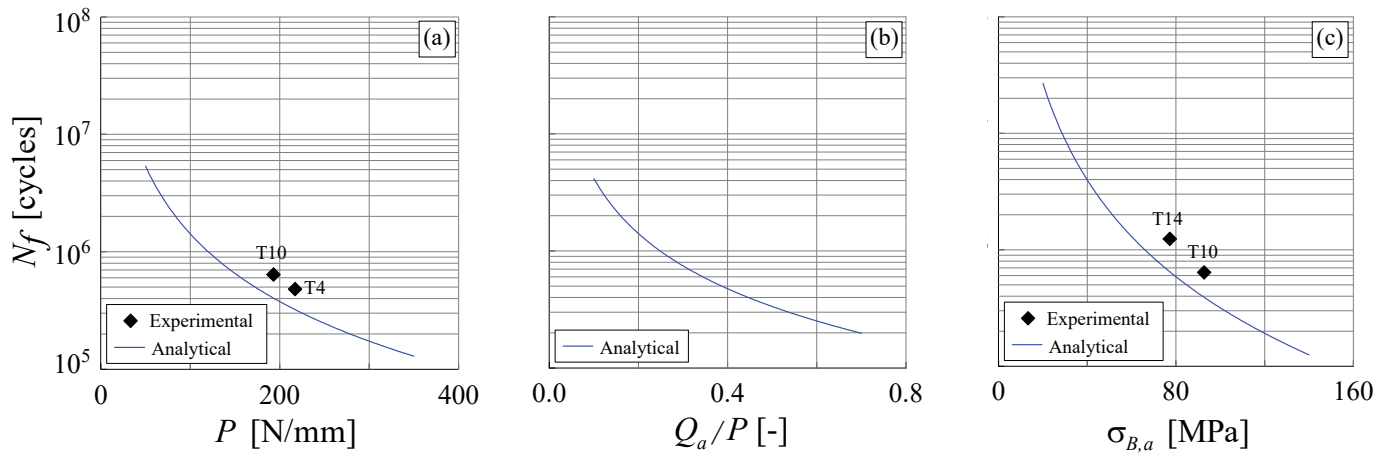


Figure 2: Fretting fatigue life as a function of: (a) the constant normal load, P ; (b) the amplitude of the cyclic tangential load, Q_a (by changing the ratio Q_a/P); and (c) the amplitude of the cyclic axial stress, $\sigma_{B,a}$.

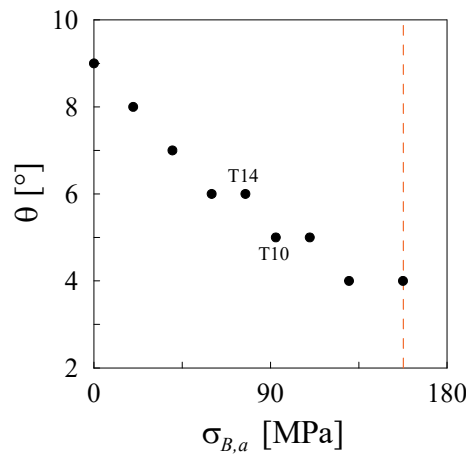


Figure 3: Crack nucleation orientation, θ , as a function of the amplitude of the cyclic axial stress, $\sigma_{B,a}$. The orange dotted line identifies the limit for the partial slip condition. The points characterised by $\sigma_{B,a}$ equal to 92.7 and 77.2 MPa correspond to the experimental configurations of test Nos T10 (reference condition) and T14, respectively.

As far as the material properties are concerned, it is interesting to examine the influence of the friction coefficient and of the grain size on both fatigue life and crack nucleation orientation. As a matter of fact, the fatigue behaviour of fretting-affected components strongly depends on these parameters, whose value is generally difficult to determine uniquely and unambiguously. In particular, there is no straightforward technique to directly measure the friction coefficient, μ , and, in the present case, it has been analytically estimated [4], starting from the measured mean value, $\mu_m=0.5$. Moreover, even the value of the average grain size, d , is not easy to determine, since it can vary with the depth, and the grains can be elongated. It is therefore necessary to find out where and which is the most appropriate size to use.

By considering all the experimental data (see Tab. 2), the effect of the friction coefficient, μ , on the fatigue life is shown in Fig. 4 (a), in which the results related to a friction coefficient of 0.5 (that is, the value of μ_m) are plotted together with those related to $\mu=0.75$ (that is, the value previously used for the methodology validation). It can be observed that a decrease of the value of the friction coefficient results in an increase of the fatigue lives (average increase of 66%), thus obtaining fewer conservative estimations. This results in a modification of the T_{RMS} value, which becomes equal to 2.35 in this case.

On the other hand, the crack nucleation orientation is almost independent of the value of the friction coefficient: in the present case, it decreases on average by only 1.1° compared to the case with $\mu=0.75$.

Further, the effect of the average material grain size, d , on the fatigue life is shown in Figs. 4 (b) and (c), in which a value half ($25 \mu\text{m}$) and double ($100 \mu\text{m}$) the experimentally measured one is considered, respectively. The fatigue life results computed in the case of $d=50 \mu\text{m}$ (that is, the value previously used for the methodology validation) are also plotted in Figs. 4 (b) and (c) for comparison. It can be observed that the fatigue life decreases by decreasing the value of the grain size,

whereas it increases as d increases. More precisely, an average variation of -55% and +174% is obtained when d is assumed equal to 25 and 100 μm , respectively. This results in a modification of the T_{RMS} value, which becomes equal to 1.99 and 3.81 in these two cases, respectively.

As far as the crack nucleation orientation is concerned, it is observed to change of about $\pm 2^\circ$ when either a value half or double the average grain size is assumed and, more precisely: a smaller value of θ is the result of the grain size reduction; conversely, when the grain size increases, an increase of θ is obtained.

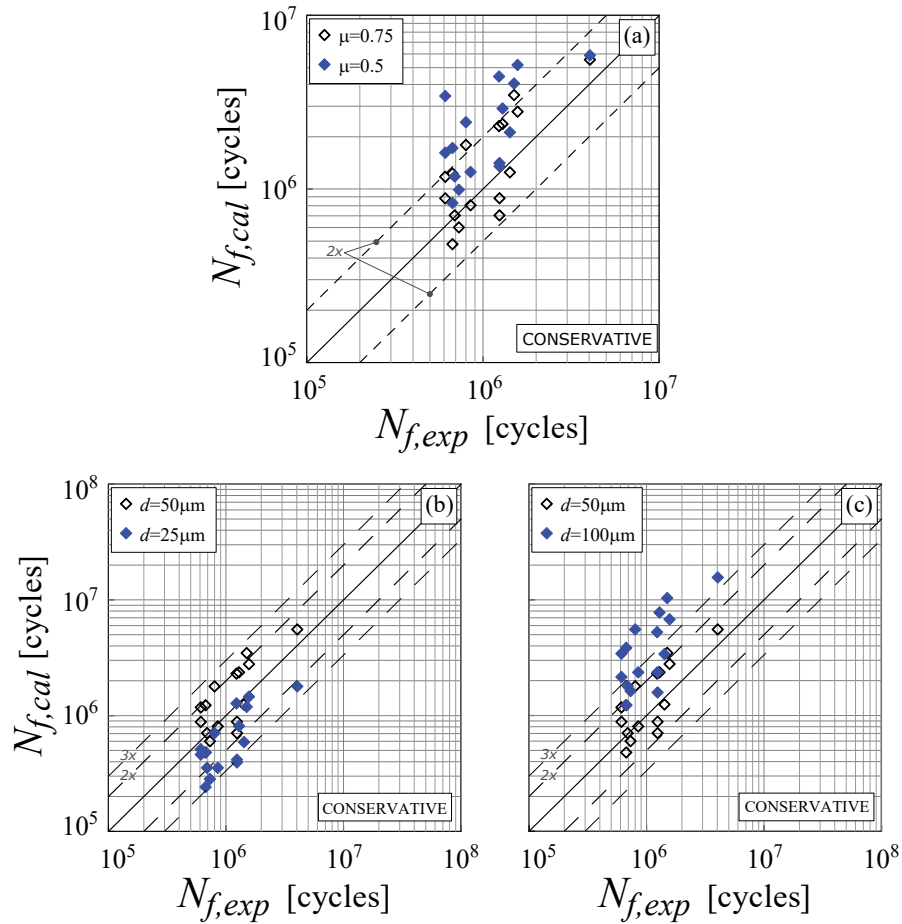


Figure 4: Analytical, $N_{f,cal}$, vs experimental, $N_{f,exp}$, fatigue life for all specimens analysed when: (a) the friction coefficient, μ , is equal to 0.75 and 0.5; (b) the average grain size, d , is equal to 50 μm and 25 μm ; and (c) d is equal to 50 μm and 100 μm .

All the parameters considered so far significantly affect the fatigue life. On the other hand, they slightly affect the crack nucleation orientation. Therefore, since the present analytical methodology underestimates the real value of the crack nucleation orientation, an additional parameter needs to be taken into account in order to try improving the estimation of θ . Such a parameter is the relative micro-slip between the contact surfaces, and it can be incorporated in the present methodology through the Ruiz parameter (which is function of both stress field and relative slip), as reported in Ref. [20]. In order to do that, the assumption that the hot-spot, H , on the contact surface is found in correspondence of the maximum value of the maximum principal stress needs to be modified. In particular, the point characterised by the maximum value of the Ruiz parameter is assumed as the hot-spot on the contact surface. Note that the hot-spot identifies the location of crack nucleation.

The results in terms of fatigue life estimations, obtained when H is assumed to be the point maximising either the maximum principal stress (that is, the location previously assumed for the methodology validation) or the Ruiz parameter, are plotted in Fig. 5. It can be observed that in this case the results in terms of fatigue life are very similar to those obtained when H is found at the contact edge, with a slight average variation of -4% towards the conservative side. In this case, the T_{RMS} is almost constant, even if a very little improvement is noted, with a new value of 1.64.

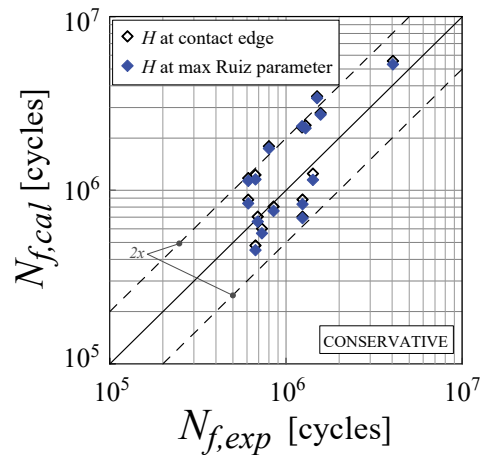


Figure 5: Analytical, $N_{f,cal}$, vs experimental, $N_{f,exp}$, fatigue life for all specimens analysed when the hot-spot is assumed as the point maximising either the maximum principal stress (H at contact edge) or the Ruiz parameter (H at max Ruiz parameter).

On the other hand, the crack nucleation orientation increases of about 7° with respect to the case when H is at the contact edge. In particular, angles ranging between 14° and 17° (see Tab. 3) are obtained when the micro-slips are taken into account in the determination of the crack nucleation location. It can be highlighted that in this case the present analytical methodology provides better estimations in terms of θ , since angles more similar to the experimental ones (whose minimum values were measured equal to 18°) are obtained.

CONCLUSIONS

In the present paper, an analytical methodology for fretting fatigue assessment of metallic structures has been employed. Such a methodology was recently proposed for the estimation of both crack nucleation orientation and fatigue life of fretting-affected components.

Firstly, a comprehensive experimental campaign available in the literature has been considered in order to validate the analytical methodology. These experimental tests were carried out on an aluminium alloy in partial slip regime, by using two cylindrical fretting pads pushed against a dog bone specimen. Satisfactory results have been obtained in terms of fatigue life estimation, with a T_{RMS} equal to 1.66. However, the computed crack nucleation orientations underestimate the measured experimental ones, ranging from 6° to 11° for the former and from 18° to 34° for the latter.

Subsequently, a parametric analysis is carried out to assess the role of different influencing factors in affecting the fretting fatigue behaviour when the above methodology is employed.

In particular, it has been observed that the input parameters related to the contact geometry (that is, the radius of the pad), the fretting loading (that is, the constant normal load, the amplitude of the cyclic tangential load, and the amplitude of the cyclic axial load) and the material properties (that is, the friction coefficient and the average grain size) significantly affect the fatigue life, whereas they only have a marginal effect on the crack nucleation orientation.

Finally, the amplitude of the relative micro-slip has been taken into account together with the stress field in the determination of the crack nucleation location on the contact surface. In this case, results in terms of fatigue life very similar to those related to the methodology validation has been obtained (with almost the same T_{RMS}), whereas the crack nucleation orientation is estimated quite similar to the minimum experimental ones.

REFERENCES

- [1] Tomlinson, J. (1927). The fretting of metals under load, *Philos. T. Roy. Soc. A*, 226(1), pp. 211-227. DOI: 10.1098/rsta.1927.0007.
- [2] Waterhouse, R., Lindley, T. (1994). *Fretting fatigue*, London, ESIS Publications.
- [3] Mindlin, R.D. (1949). Compliance of Elastic Bodies in Contact, *J. Appl. Mech.-T. ASME*, 16(3), pp. 259-268. DOI: 10.1115/1.4009973
- [4] Hills, D.A., Nowell, D. (1994). *Mechanics of Fretting Fatigue*, Netherlands, Springer.



- [5] Bentahar, M., Benzaama, H., Noureddin, M. (2021). Numerical modeling of the contact effect on the parameters of cracking in a 2d fatigue fretting model, *Frat. Integrità Strutt.*, 15(57), pp. 182-194. DOI: 10.3221/IGF-ESIS.57.15.
- [6] Hamadouche, F., Benzaama, H., Mokhtari, M., Tahar, M.A. (2021). Influence of contact parameters in fretting-fatigue contact 3D problems, *Frat. Integrità Strutt.*, 15(55), pp. 228-240. DOI: 10.3221/IGF-ESIS.55.17.
- [7] Vantadori, S., Vázquez Valeo, J., Zanichelli, A., Carpinteri, A., Luciano, R. (2022). Structural integrity of shot peened Ti6Al4V specimens under fretting fatigue, *Int. J. Fracture*, 234, 1-2, pp. 45-55. DOI: 10.1007/s10704-021-00523-0
- [8] Majzoobi, G.H., Abbasi, F. (2017). On the effect of contact geometry on fretting fatigue life under cyclic contact loading, *Tribol. Lett.*, 65, 125. DOI: 10.1007/s11249-017-0906-9.
- [9] Vantadori, S., Zanichelli, A., Erena, D., Vázquez, J. (2023). Effect of rolling on fretting fatigue assessment of cylindrical contact in partial slip regime, *Trib. Int.*, 188, 108772. DOI: 10.1016/j.triboint.2023.108772
- [10] Duquette, D.J. (1980). Role of cyclic wear (fretting) in fatigue crack nucleation in steels, *Energy Technol.*, pp. 213-218.
- [11] Hills, D.A. (1994). Mechanics of fretting fatigue, *Wear*, 175(1-2), pp. 107-113. DOI: 10.1016/0043-1648(94)90173-2.
- [12] Su, Y., Rui, S.S., Han, Q.N., Shang, Z.H., Niu, L.S., Li, H., Ishikawa, H., Shi, H.J. (2022). Estimation Method of Relative Slip in Fretting Fatigue Contact by Digital Image Correlation, *Metals*, 12(7), 1124. DOI: 10.3390/met12071124.
- [13] Chen, Q., Xu, Y., Zheng X. (2024). Microstructure-sensitivity of CPFEM models on fretting fatigue crack initiation of AA2024-T351 alloy, *J. Constr. Steel Res.*, 222, 108971. DOI: 10.1016/j.jcsr.2024.108971.
- [14] Santos, L.M.S., Borrego, L.P., Ferreira, J.A.M., de Jesus, J., Costa, J.D., Capela, C. (2019) Effect of heat treatment on the fatigue crack growth behaviour in additive manufactured AISI 18Ni300 steel, *Theor. Appl. Fract. Mec.*, 102, pp. 10-15. DOI: 10.1016/j.tafmec.2019.04.005.
- [15] Bartolomei, M.L., Kudryashev, I.S., Sabirov, R.R., Korsunsky, A.M. (2025). Numerical study of residual stress fields after double-sided symmetric laser shock peening of blade edge, *Fractur. Struct. Integr.*, 19 (72), pp. 26–33. DOI: 10.3221/IGF-ESIS.72.03.
- [16] Torres Duarte, L.M., Domínguez Almaraz, G.M., Venegas Montaña, H.M. (2024). Ultrasonic fatigue testing of AISI 304 and 316 stainless steels under environmental and immersion conditions, *Fractur. Struct. Integr.*, 18(68), 175–185. DOI: 10.3221/IGF-ESIS.68.11.
- [17] Rustamov, I., Zhang, G., Skotnikova, M., Wang, Y., Wang, Z. (2019). Fretting wear behavior and damage mechanisms of inconel X-750 alloy in dry contact condition, *J. Tribol.*, 141(4), 041603. DOI: 10.1115/1.4042038
- [18] Song, J., Yuan, H., Schinow, V. (2019). Fretting corrosion behavior of electrical contacts with tin coating in atmosphere and vacuum, *Wear*, 426-427, pp. 1439-1445. DOI: 10.1016/j.wear.2018.11.024.
- [19] Li, Y., Xie, G., Sun, X., Jingcao, C., Wu, X., Zhang, Y., Yu, C., Du, P. (2025). A review on fretting wear/fatigue behavior, protective measures, and application examples of typical alloy materials, *Proc. Inst. Mech. Eng. J: J. Eng. Tribol.* DOI: 10.1177/13506501241313249.
- [20] Zanichelli, A., Ronchei, C., Scorza, D., Vantadori, S. (2022). Influence of hot-spot on crack path and lifetime estimation of fretting-affected steel components, *Theor. Appl. Fract. Mec.*, 121, 103467. DOI: 10.1016/j.tafmec.2022.103467.
- [21] Araújo, J.A., Nowell, D., Vivacqua, R.C. (2004). The use of multiaxial fatigue models to predict fretting fatigue life of components subjected to different contact stress fields. *Fatigue Fract. Eng. Mater. Struct.*, 27(10), pp. 967-978. DOI: 10.1111/j.1460-2695.2004.00820.x.
- [22] Hertz, H. (1896). *Miscellaneous Paper by Heinrich Hertz*, New York, Macmillan & Co.
- [23] Araújo, J.A., Almeida, G.M.J., Ferreira, J.L.A., da Silva, C.R.M., Castro, F.C. (2017). Early cracking orientation under high stress gradients: The fretting case. *Int. J. Fatigue*, 100, pp. 611-618. DOI: 10.1016/j.ijfatigue.2016.12.013.
- [24] Carpinteri, A., Boaretto, J., Fortese, G., Giordani, F., Rodrigues, R.I., Iturrioz, I., Ronchei, C., Scorza, D., Vantadori, S., Zanichelli, A. (2018). Welded joints under multiaxial non-proportional loading, *Theor. Appl. Fract. Mec.*, 93, pp. 202-210. DOI: 10.1016/j.tafmec.2017.08.004.
- [25] Vantadori, S., Ronchei, C., Scorza, D., Zanichelli, A., Carpinteri, A. (2021). Fatigue behaviour assessment of ductile cast iron smooth specimens, *Int. J. Fatigue*, 152, 106459. DOI: 10.1016/j.ijfatigue.2021.106459.